

# Development and simulation of a passive upper extremity orthosis for amyoplasia

Erik F Jensen<sup>1</sup>, Joakim Raunsbæk<sup>1</sup>, Jan N Lund<sup>1</sup>, Tariq Rahman<sup>2</sup>, John Rasmussen<sup>3</sup> and Miguel N Castro<sup>3</sup> 

## Abstract

**Introduction:** People who are born with arthrogryposis multiplex congenita are typically not able to perform activities of daily living (ADL) due to decreased muscle mass, joint contractures and unnatural upper extremity positioning. They are, therefore, potential users of an assistive device capable of aiding in ADL and increasing their independence. A passive orthosis can support the weight of their arm against gravity, allowing them to perform movements with less effort.

**Methods:** This study presents a prototype design with four degrees-of-freedom that uses musculoskeletal modelling to optimize the stiffness of the springs in the device to partially gravity balance the upper extremity while compensating for the usual internally rotated glenohumeral joint. A single subject-specific musculoskeletal model was developed to simulate the effects of the passive orthosis during 10 static postures during ADL.

**Results:** For a given configuration using a mono- and a bi-articular spring, the simulations showed that spring stiffnesses of  $400 \text{ Nm}^{-1}$  and of  $1029 \text{ Nm}^{-1}$ , respectively, were able to lower the maximal muscle activity estimated by the musculoskeletal model to a level in which the 10 postures can be realized.

**Conclusion:** By augmenting residual muscle strength with a partially gravity-balanced passive orthosis, ADLs may be achievable for people with arthrogryposis multiplex congenita.

## Keywords

Passive orthosis, partial gravity balance, upper extremity, arthrogryposis, amyoplasia, musculoskeletal modelling

Date received: 1 August 2017; accepted: 30 January 2018

## Introduction

The movement capabilities of the upper extremities are essential for independence.<sup>1</sup> Arthrogryposis multiplex congenita (AMC) is a disorder in which people often lack these movement capabilities. This disorder is classified as a heterogeneous group of diseases with more than 300 different conditions, with the main characteristic involving multiple congenital joint contractures.<sup>2,3</sup> The prevalence of AMC is 1 in 3000 live births.<sup>4</sup> The most common type of AMC is amyoplasia, which is a combination of decreased muscle mass and joint contractures with some distinct characteristics; typically the shoulders are adducted and internally rotated, the elbows are extended and the wrists are flexed and ulnarly deviated.<sup>3–6</sup> However, these anatomical characteristics might differ between subjects.<sup>5</sup> Decreased muscle mass is usually found in the deltoids, the biceps brachii and the brachialis muscles.<sup>3</sup>

The combination of contractures and muscular weakness makes activities such as self-feeding, reaching the face and handling objects difficult or impossible.<sup>7</sup> The occurrence of amyoplasia is sporadic, and the genetic cause is still unknown.<sup>8,9</sup> The exact aetiology is also unknown, but among a number of factors, foetal akinesia is a prevalent factor in developing AMC.<sup>5</sup>

Treatment of subjects with amyoplasia is performed in different ways, primarily to improve the quality of

<sup>1</sup>Department of Health Science and Technology, Aalborg University, Aalborg, Denmark

<sup>2</sup>Department of Biomedical Research, Nemours/Alfred I DuPont Hospital for Children, Wilmington, DE, USA

<sup>3</sup>Department of Materials and Production, Aalborg University, Aalborg, Denmark

### Corresponding author:

Miguel N Castro, Department of Materials and Production, Aalborg University, Fibigerstraede 16, 9220 Aalborg East, Denmark.  
Email: mnc@make.aau.dk



life and enable activities of daily living (ADL).<sup>3,9</sup> Physical therapy, stretching and splinting are used to mobilize the joints and stimulate muscle growth.<sup>6,10</sup> Surgery is another treatment method primarily targeting the lack of elbow flexion.<sup>4</sup> Concerning passive elbow flexion, surgical procedures have shown excellent results in regard to increased passive motion and improved independence for feeding. Due to lack of active elbow flexion, performing ADL still requires compensatory techniques such as using the assistance of the opposite arm or propping the arm against a table.<sup>11</sup> The outcome of surgical procedures intended to improve active elbow flexion are encouraging. However, according to Lahoti and Bell,<sup>12</sup> a progressive increase in flexion deformity and decrease in the arc of flexion were observed over time. As an alternative to the therapeutic and surgical methods, there has been moderate research in assistive devices, such as orthoses, that are able to compensate for the muscular weakness of the upper extremities and assist the subject in performing ADL.<sup>13</sup> Passive devices are based on the static balancing principle by using potential elastic energy stored in mechanical components such as zero-free-length springs.<sup>13</sup> These orthoses may be used by people with AMC to aid in ADL. Orthoses allow for the increased use of the arms, thus aiding in the development of muscle. Kroksmark et al.<sup>14</sup> emphasize the importance of muscle development over treatment of contractures, since the muscular strength is more important for motor function. This may be achieved using a partially gravity-balanced system.<sup>15</sup>

There are different commercially available passive orthoses that can balance the arm in a wide range of configurations. An example of a passive orthosis is the Wilmington Robotic Exoskeleton (WREX).<sup>7</sup> The WREX is a four degrees-of-freedom (DOF) passive device using parallelograms to gravity balance the upper limb. Another device is A-gear, relying on multi-articular springs to balance two serial linkages.<sup>16</sup> The latter approach is based on a recent formulation called the stiffness matrix approach which is a planar energy-based method.<sup>17</sup> This method was extended from polar coordinates to Cartesian coordinates by Lustig et al.<sup>18</sup> The A-gear consists of one mono-articular spring spanning the elbow joint and one bi-articular spring spanning both shoulder and elbow joints.<sup>16</sup> However, a limitation associated with this fully gravity-balanced configuration is that the springs' attachments on the lower arm are determined by the length and masses of both upper- and lower arm segments which makes it too bulky to fit underneath clothing.<sup>19</sup>

In the present work, a subject-specific passive orthosis prototype with four DOF was designed to bring the internally rotated glenohumeral joint into neutral position while providing assistance through an increased

range-of-motion for subjects with amyoplasia. Similar to the A-gear, the orthosis uses two zero-free-length springs to counterbalance gravity in different upper extremity configurations, plus an extra shoulder internal/external rotation assistive spring. In order to improve the compactness of the orthosis, musculoskeletal modelling was used to simulate a partially gravity-balanced configuration of the orthotic device taking the subject-specific muscular weakness into account. Therefore, the characteristics of an idealized amyoplasia patient were simulated in the model. The muscle recruitment for sustaining a given set of static postures was later assessed using the model with and without a designed orthotic device. Each spring stiffness was selected by minimising the maximum muscle activation (MMACT) required to sustain those postures. The results will be presented and discussed with the purpose of setting guidelines for further studies.

## Methods

Anthropometric data from one healthy male subject (age: 26, mass: 70 kg, height: 178 cm) were acquired in the current study with the aim of setting the musculoskeletal modelling background. The subject was initially equipped with 20 reflective skin markers attached to the pelvis, trunk, shoulder and right arm. The position of the reflective markers was recorded using an eight-camera motion capture system (Qualisys AS, Gothenburg, Sweden) at a sampling frequency of 100 Hz. Kinematic data were analysed using the AnyBody Modelling System 6.1 (AMS) (AnyBody Technology, Aalborg, Denmark), and a static trial was conducted in neutral position as reference to scale the model to the subject.

### Musculoskeletal modelling

In order to simulate the effects of the orthosis on the human body, an upper extremity musculoskeletal model was created in AMS from the built-in repository v1.6.3. The model is based on the lumbar spine data from the work of de Zee et al.,<sup>20</sup> while the shoulder, upper and lower arm data belong to the work of the Delft Shoulder Group.<sup>21–23</sup> The musculoskeletal model comprises eight DOF: three DOF at the sternoclavicular joint, three DOF at the glenohumeral joint and two DOF at the elbow joint. The static trial was used to geometrically scale the model to the subject by the method of Andersen et al.<sup>24</sup> as presented in Figure 1. This is a local optimization-based method which minimizes the least-square differences between marker trajectories and the markers defined on the musculoskeletal model. In total, the musculoskeletal model included 140 simple muscle model elements.

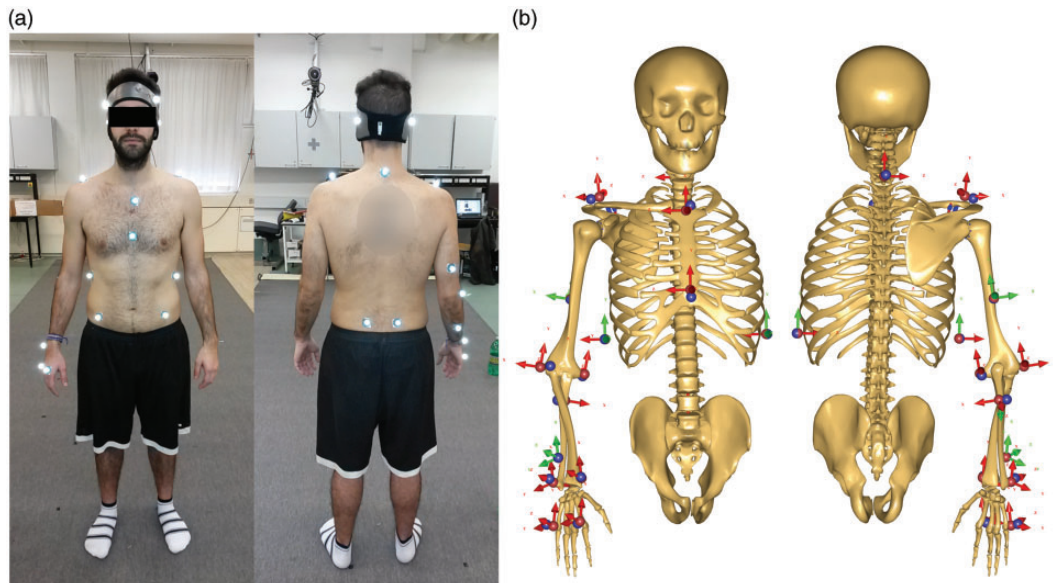


**Figure 1.** (a) The kinematic data collected during a static trial from the reflective markers set constant trajectories was used to geometrically scale the musculoskeletal model. (b) The captured markers (blue coloured) were approximated by each respective marker (red coloured). The method of Andersen et al.<sup>24</sup> helps optimising the green-arrowed markers in the model which do not belong to a specific bony landmark.

Their nominal strength was scaled according to a Length-Mass-Fat Scaling law,<sup>25</sup> which is a general scaling method capable of estimating the nominal strength from the body segments' mass and length, with the inclusion of a fat percentage based on the body height-weight ratio. In AMS, the internal forces and moments from muscles and joints are found by formulating a complete set of Newton-Euler equations for dynamic equilibrium, relating all segments' inertial properties within the model.<sup>26</sup> The inverse dynamics analysis solves those equations from prior results obtained in the kinematic analysis in which the state of the system obtained for each time instant of the recorded motion. The number of muscle elements is far greater than the number of DOFs in the model, rendering the equilibrium equations under-determined – this is known as the redundancy problem of the muscle recruitment.<sup>27</sup> The physiological mechanism of muscle activation is controlled by the central nervous system but is still not well understood. Therefore, the muscle recruitment in musculoskeletal modelling is typically based on an optimality condition, where the central nervous system minimizes the loads across the different muscles. The min/max muscle recruitment criterion developed by Rasmussen et al.<sup>27</sup> was used in this study, and it distributes the muscle forces in such a way that the overall MMACT is minimized. The min/max criterion is suitable for this study since, in maximal effort tasks, it delays fatigue by ensuring maximal muscle synergism.

In order to obtain realistic posture inputs for the musculoskeletal model, motion capture data for 10 different ADL were obtained. These ADL motions were selected from those suggested by Rosen et al.<sup>28</sup> and a representative posture of each was selected. An unconstrained segment usually requires three reflective markers attached to describe its motion, thus resulting in nine DOF. This introduces over-determinacy because a segment only has six DOF. Furthermore, the joint constraints imposed by the human body further increase that gap leading to an over-determinacy problem. This over-determinacy introduced by the marker coordinates was solved using the method of Andersen et al.<sup>29</sup> The 10 different postures are illustrated in Figure 2, and these were simulated by the musculoskeletal model. The majority of these tasks usually involve the hand reaching a point in space, grasping an object and then controlling and orienting the object until the task is completed.<sup>30</sup> Examples of important ADL include feeding and personal hygiene, which includes touching the face and head.<sup>31</sup> Being able to perform these tasks can provide more independence to the user as well as improve their quality of life.

The output measure in the current study is based on the MMACT, which determines whether the muscle system is able to produce the joint moments required to balance the system for each static posture. The muscle activity is the ratio between required produced force and each muscle's nominal strength. If the MMACT is greater than one for any given muscle,

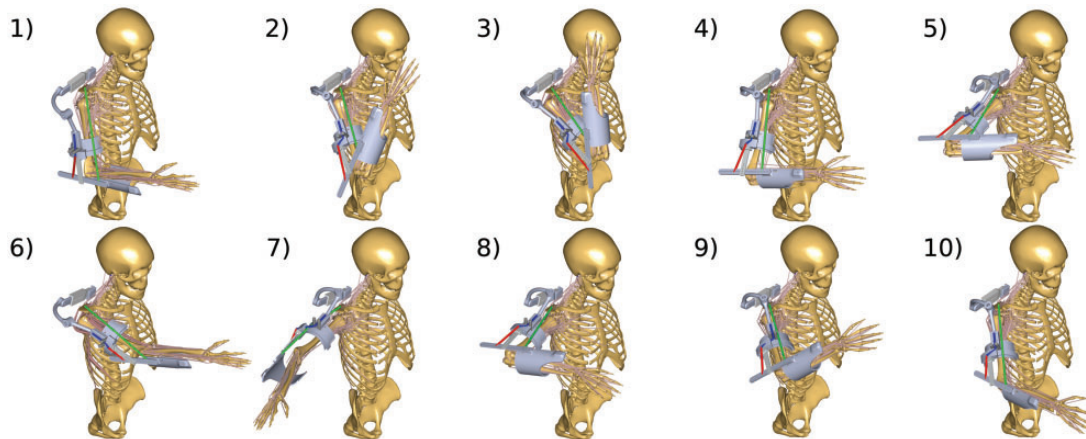


**Figure 2.** The 10 different postures used for the inverse dynamic analyses.

there is insufficient strength to maintain the posture. However, in the case of a simulated disabled subject unable to use a given DOF, all muscles actuating that DOF are removed from the model. In order to enable the inverse dynamic solver to establish equilibrium, an additional artificial ‘diagnostic’ muscle is added to balance the specific DOF. This ‘diagnostic’ muscle is a torque provider which will be recruited whenever the required DOF torque is beyond what is provided by the orthosis in order to attain the required posture. For the specific case of amyoplasia, both elbow and glenohumeral flexion are compromised as reported by Kowalczyk and Feluś.<sup>3</sup> Therefore:

All muscles with a positive contribution to elbow flexion and the anterior deltoid were disabled and substituted by a very weak elbow flexion torque provider. The joint and muscle contractures were not included in the model.

The inverse dynamics analyses were performed for static postures only.

### Orthosis modelling

A prototype of a passive orthosis, using zero-free-length springs, was designed to assist in the performance of ADL. In light of what was previously mentioned, the orthosis must be able to support and follow the movements of the shoulder and elbow. The movements will be aided by mechanical springs capable of counterbalancing gravity. In addition, an extra spring will aid the external rotation of the user’s glenohumeral joint, thus bringing the humerus into a more neutral position. A secondary goal is that the motion enabled by the orthosis can aid in the promotion of muscle development.<sup>6,32</sup> The orthosis CAD model can be seen in Figure 3.

The system combining the human arm and the orthosis is shown schematically in Figure 4. The inner lines represent the human arm, while the outer lines represent the orthosis. The orthosis is in parallel with the upper extremity supporting its anatomical glenohumeral joint, represented as a spherical joint with three DOF ( $\theta_{a1}$ ,  $\theta_{a2}$ ,  $\theta_{a3}$ ), and elbow joint which is represented with one DOF. The orthosis itself is composed of five revolute joints:  $\theta_{o1}$  allows for elevation/depression of the shoulder; the three revolute joints  $\theta_{o2}$ ,  $\theta_{o3}$  and  $\theta_{o4}$  represent the three DOFs of the shoulder, abduction/adduction, flexion/extension and internal/external rotation, respectively; and the connection between the upper arm shell and the forearm shell is created by a revolute joint  $\theta_{o5}$ , which represents elbow flexion/extension. A gimbal lock occurs in this shoulder mechanism when the shoulder abducts more than  $90^\circ$  flexion. However, a study by Buckley et al.<sup>33</sup> has found that the required shoulder abduction for ADL is usually less than  $90^\circ$ . Dunning and Herder<sup>13</sup> have also suggested that a possible design could be to neglect the full vertical range-of-motion of the shoulder, focusing only on the support of the most essential daily tasks. The orthosis was created to function within this recommended range. The whole system is supported by: a bi-articular spring,  $S_1$ , originating above the glenohumeral joint and inserting on forearm link spanning both glenohumeral and elbow joints; a mono-articular spring,  $S_2$ , located along the humerus and posterior to the elbow assisting the extension. On the humeral-lateral aspect of the orthosis, a rail is attached, whereas the slider is attached to the elbow joint. As the shoulder internally and externally rotates, the slider follows accordingly. Considering that one of the most common patterns of deformity in the upper extremity due to amyoplasia is the internal rotation of the shoulder,<sup>9</sup> the purpose of this mechanism is to aid the alignment of the shoulder into a neutral position.



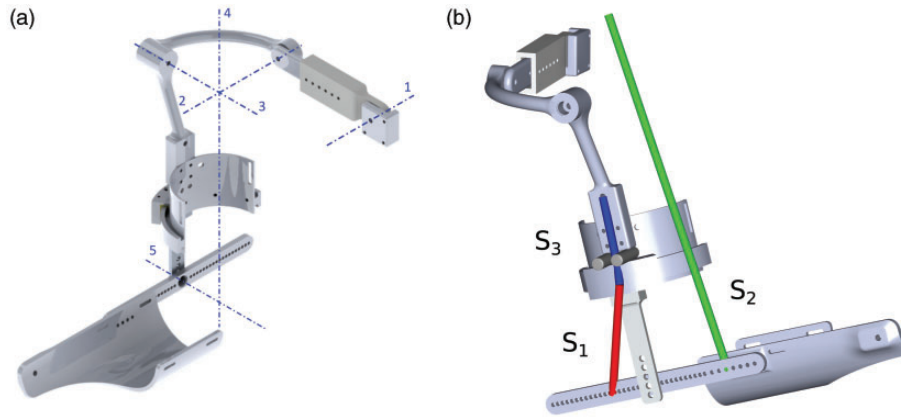


**Figure 3.** (a) Full orthosis DOFs: 1. Shoulder elevation/depression; 2. Shoulder abduction/adduction; 3. Shoulder flexion/extension; 4. Shoulder internal/external rotation; 5. Elbow flexion/extension. (b) Full orthosis springs configuration: mono-articular spring ( $S_1$ ); bi-articular spring ( $S_2$ ); internal/external rotation assistive spring ( $S_3$ ).

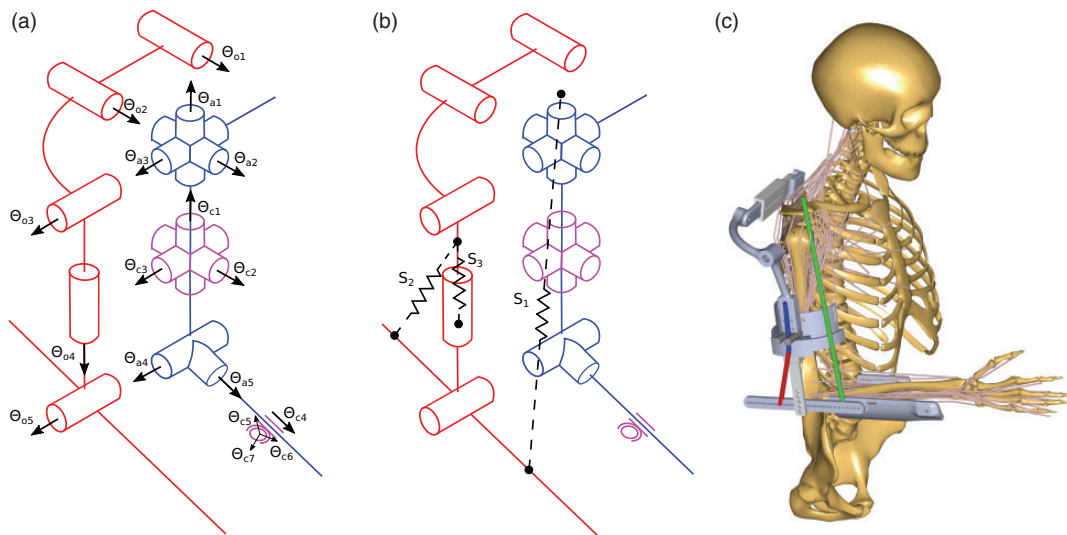


**Figure 4.** (a) Schematic of the musculoskeletal model (inner lines) and orthosis model (outer lines) system. The joints connecting both models are illustrated by the purple symbols. All DOF and mechanical joint angles are represented by black arrows. (b) The three springs are presented by dashed lines. (c) The orthosis CAD model connected to the musculoskeletal model as described.

The assistive spring,  $S_3$ , is attached using two parallel points located on the lateral aspect of the humerus and the slider. On the humerus, anteriorly and posteriorly located between the attachments, there are two pulleys. As the user internally or externally rotates the humerus, the pulleys act on the spring, increasing the force and tension as the slider moves further, bringing and aligning the humerus into a more neutral position.<sup>9</sup>

To determine whether the orthosis is capable of fulfilling its intended function, the interaction between the orthosis and the human body has to be examined. In this study, the essential aspect of the musculoskeletal modelling is the simulation of how the human body is affected by the external forces produced by the orthosis

and gravity. The CAD model of the orthosis along with the mass properties of the individual parts of the orthosis were imported into AMS. To establish the human–orthosis interaction system, the orthosis was attached to the musculoskeletal model through three predefined reference nodes located on the thorax, the humerus and the ulna. The attachments between the human arm and the orthosis were defined and modelled as mechanical joints. The upper arm attachment was modelled as a spherical joint,  $\theta_{c1}$ ,  $\theta_{c2}$ ,  $\theta_{c3}$  and the forearm attachment as a trans-spherical joint, with three rotations  $\theta_{c5}$ ,  $\theta_{c6}$ ,  $\theta_{c7}$  plus a translational DOF  $\theta_{c4}$  as illustrated by the symbols drawn in the middle of each segment of the musculoskeletal model in Figure 4.

### Simulation specifications

In order to investigate a suitable and favourable spring configuration that yields the lowest average MMACT for the 10 postures, 10 corresponding numerical studies were conducted. Three different springs (Figure 4) were available for load balancing. The ranges of spring stiffnesses and initial locations for the parameter study were determined by the method of Lustig et al.<sup>18</sup> For the bi-articular spring, the applied stiffness range 0 to  $700 \text{ Nm}^{-1}$ , and for the mono-articular spring, it was 0 to  $1200 \text{ Nm}^{-1}$ . The ranges of the two springs were covered in 15 steps in the parameter study, resulting in 225 different combinations of spring configurations for each of the 10 postures. Because Lustig et al.'s method is two-dimensional, the stiffness of the internal/external rotation spring was merely chosen from available zero-free-length springs (Synthetic Polyisoprene, Jaeco Orthopedic, Arkansas, USA) to  $84 \text{ Nm}^{-1}$  and remained unchanged.

The ideal forearm attachment points for the mono- and bi-articular spring were calculated to 10.25 cm anterior to the elbow joint and 7.7 cm posterior to the elbow joint, respectively. However, in the interest of

compactness, the spring attachments site for the bi-articular spring was relocated to 5 cm anteriorly to the elbow and the mono-articular spring was attached 7.2 cm posteriorly to elbow. This creates an imbalance, but the goal was to investigate whether the arm could still be sufficiently gravity balanced to allow the subject to perform ADL with the residual muscle function (typical patients have some remaining glenohumeral and elbow flexor strength).

A schematic of the mechanism and respective spring configuration used in the present study can be seen in Figure 5, while the values used and calculated can be found in Table 1. For every step of each parameter study, an inverse dynamics analysis was performed and an MMACT value was obtained. To assess the stiffness for both mono- and bi-articular springs that would yield the lowest MMACT in the biomechanical model, the average MMACT across all 10 postures was calculated and plotted for each of the 225 spring configurations. In addition, the five different global strength factors (0.2, 0.4, 0.6, 0.8 and 1.0) were pre-multiplied with the nominal strength of each muscle element in the biomechanical model in order to test whether the strength would influence the results.

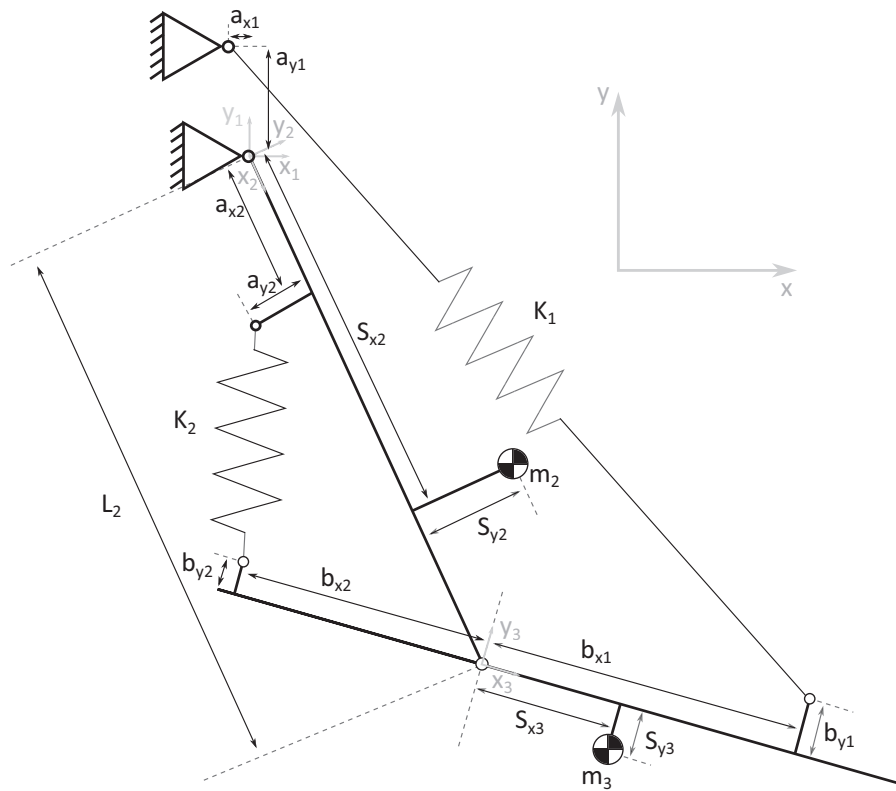


**Figure 5.** Schematic of the mechanism with the representation of stiffness matrix inputs for the Cartesian coordinates formulation of Lustig et al.<sup>18</sup>

**Table 1.** The calculated spring stiffnesses and spring placements using the method of Lustig et al.,<sup>18</sup> the six values above the line are calculated, while the values below it are set to constant values.

| Parameters                 | Values  |
|----------------------------|---------|
| $a_{x1}$ (m)               | 0.0000  |
| $b_{x1}$ (m)               | 0.1026  |
| $b_{y1}$ (m)               | 0.0009  |
| $b_{x2}$ (m)               | -0.077  |
| $b_{y2}$ (m)               | -0.0006 |
| $k_1$ ( $\text{Nm}^{-1}$ ) | 382.15  |
| $k_2$ ( $\text{Nm}^{-1}$ ) | 756.00  |
| $a_{y1}$ (m)               | 0.0700  |
| $a_{x2}$ (m)               | 0.0920  |
| $a_{y2}$ (m)               | 0.0000  |
| $m_2$ (kg)                 | 2.2940  |
| $m_3$ (kg)                 | 1.6820  |
| $L_2$ (m)                  | 0.2800  |
| $s_{x2}$ (m)               | 0.1275  |
| $s_{y2}$ (m)               | 0.0000  |
| $s_{x3}$ (m)               | 0.1662  |
| $s_{y3}$ (m)               | -0.0011 |

## Results

The typical surface profile of the average MMACT, as can be seen in Figure 6, was characterized by a valley towards the minimum value, separating two distinct domains: a very steep domain characterized by the over-activation of the elbow flexor ‘diagnostic’ torque provider and a second domain characterizing the recruitment of the elbow extensor muscles. Both domains are direct responses to the dominance of either the mono-articular spring over the bi-articular spring and vice versa, respectively, always accounting with the strength of the muscle elements in the model. Moreover, the strength of the model did not influence the result of stiffness for the optimal springs’ stiffness configuration. The stiffness configuration yielding the lowest MMACT was composed of mono-articular spring stiffness of  $1029 \text{ Nm}^{-1}$  and a bi-articular spring stiffness of  $400 \text{ Nm}^{-1}$ .

The MMACT was then simulated for the 10 posture cases with and without the orthosis for the previously obtained spring configuration yielding in the lowest average MMACT. The results regarding these 10 parameter studies are shown in detail in Table 2. The table shows that the MMACT was greater than 1 in 7 of the 10 postures, when the model was not wearing the

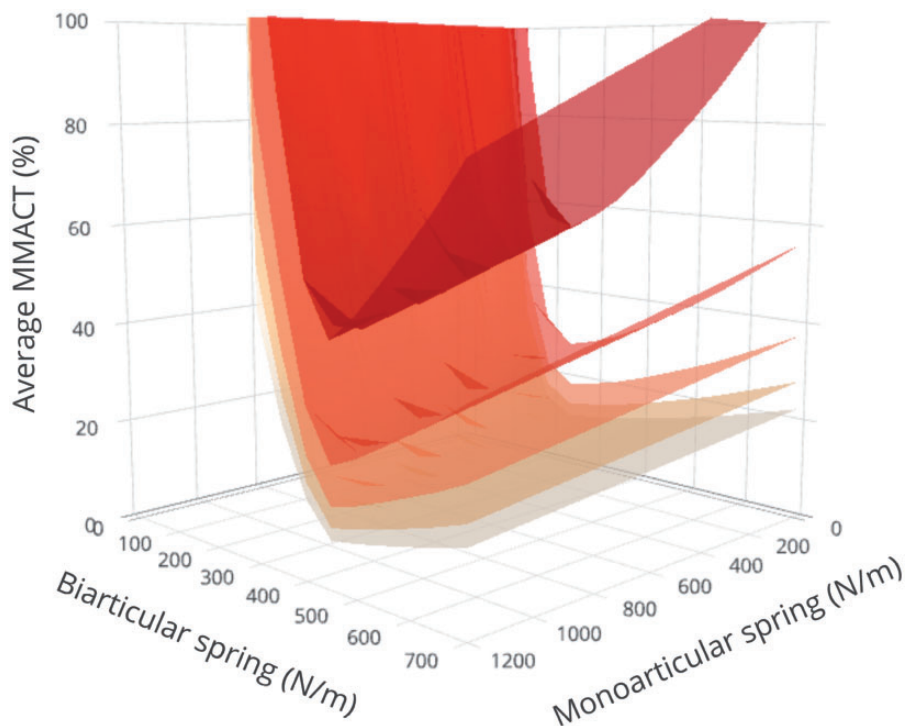


**Figure 6.** Graph showing the average MMACT for all 10 postures with different spring configurations. Layers are representing different muscle strength configurations of the muscles. The lowest layer corresponds to a global strength factor of 1 – no change – while the increasing surfaces represent consecutive strength decrements of 0.2 units, thus: 0.8, 0.6, 0.4 and 0.2. MMACT: minimising the maximum muscle activation.

**Table 2.** The maximal muscle activation values for each of the 10 different postures, with and without the optimal orthosis. When the MMACT is greater than 1 for any given muscle, there is insufficient strength to sustain the posture.

| Posture | No orthosis (MMACT) | Orthosis (MMACT) |
|---------|---------------------|------------------|
| 1       | 26.81               | 0.07             |
| 2       | 0.10                | 0.08             |
| 3       | 0.14                | 0.09             |
| 4       | 17.15               | 0.07             |
| 5       | 2.85                | 0.08             |
| 6       | 5.53                | 0.21             |
| 7       | 1.09                | 0.06             |
| 8       | 0.10                | 0.08             |
| 9       | 10.76               | 0.09             |
| 10      | 21.21               | 0.06             |

MMACT: minimising the maximum muscle activation.

orthosis, which means that model would not be able to attain the posture. While wearing the orthosis the model could attain all postures.

## Discussion

In the present study, a musculoskeletal model simulating amyoplasia of a hypothesized disabled subject with and without the orthosis was used. The spring configuration found by the use of a parameter study showed that on average a mono-articular spring stiffness of  $1029 \text{ Nm}^{-1}$  and a bi-articular spring stiffness of  $400 \text{ Nm}^{-1}$  yielded the lowest average MMACT for the 10 postures. The orthosis of the current study with the abovementioned stiffness configuration was able to lower the MMACT for all 10 postures. However, postures 2, 3 and 8 did not cause any muscle over-activation even without wearing the orthosis. This might result from the fact that inverse dynamics analyses were performed on static postures instead of dynamic motion. The results support the idea that a partially gravity balanced device might still be used for arm assistance of disabled users. In comparison to the stiffness matrix approach suggested by Lustig et al.<sup>18</sup> which, according to Dunning and Herder,<sup>19</sup> is too bulky to fit underneath clothing, these results suggest the potential for a more compact device. This not only shows a step forward towards compactness but also shows the opportunity for creating devices that could exploit some of the residual muscle function to compensate for the kinetic imbalance, thus promoting muscle growth and rehabilitation of these users.

In order to imitate amyoplasia, several assumptions were made regarding the musculoskeletal model. Zhou et al.<sup>34</sup> have shown that a specialized model can be used to design different types of exoskeletons based on

different neuromuscular conditions. The specific muscles affected may differ between different subjects due to amyoplasia being heterogeneous and very individual.<sup>5</sup> The model can potentially enable the adjustment of the strength of specific muscle elements, making the model subject-specific, thus optimizing the stiffness of the springs to the user. The musculoskeletal model does not account for the contractures typically seen in amyoplasia, which may have produced different results. These contractures could have been modelled as passive stiffness in the joints. The muscles in the model were modelled with constant nominal strength, whereas the Hill's muscle model is a more realistic representation in which force-length and force-velocity relationships can be included, thus making room for more muscle parameter adjustments.<sup>35,36</sup> With the consideration of these factors, further developments should validate the effectiveness of the orthosis, for example, by the use of the method of Castro et al.,<sup>37</sup> enabling the simulation of the full reachable workspace and investigating whether it increases by wearing the orthosis model.

## Conclusion

The current study found that musculoskeletal modelling may be a useful tool to calculate spring stiffness for partially gravity-balanced devices. This method may enable identification of spring stiffness for subject-specific orthotic devices that would allow for the performance of ADL with the potential to act as a rehabilitation device. Further studies should implement subject-specific strength measurements from a user with amyoplasia, such that it reliably represents the subject, and use dynamic motions to test the effect of the orthotic device of its user. Furthermore, the parameter study can be extended, such that spring locations can also be optimized to find the optimal relationship between spring location and spring stiffness for the best performing device. Ideally, in the future, individual muscles may be targeted, thus opening a window for the development of orthoses, thereby enhancing treatment of amyoplasia.

## Declaration of conflicting interests

The author(s) declared no potential conflicts of interest with respect to the research, authorship, and/or publication of this article.

## Funding

The author(s) disclosed receipt of the following financial support for the research, authorship, and/or publication of this article: This work was performed within the strategic platform for research and innovation Patient@Home (www.patientathome.dk), which is supported by the Danish Agency for Science, Technology and Innovation.



## Guarantor

MNC.

## Contributorship

EFJ, JR and JNL researched literature and conceived the study. All authors were involved in the model development. EFJ, JR and JNL wrote the first draft of the manuscript. All authors reviewed and edited the manuscript and approved the final version of the manuscript.

## ORCID iD

Miguel N Castro  <http://orcid.org/0000-0001-5137-0368>

## References

- Maciejasz P, Eschweiler J, Gerlach-Hahn K, et al. A survey on robotic devices for upper limb rehabilitation. *J Neuroeng Rehabil* 2014; 11: 1–29.
- Hall JG, Aldinger KA and Tanaka KI. Amyoplasia revisited. *Am J Med Genet Part A* 2014; 164: 700–730.
- Kowalczyk B and Feluś J. Arthrogryposis: an update on clinical aspects, etiology, and treatment strategies. *Arch Med Sci* 2016; 1: 10–24.
- Bamshad M, Van Heest AE and Pleasure D. Arthrogryposis: a review and update. *J Bone Joint Surg Am* 2009; 91: 40–46.
- Bernstein RM. Arthrogryposis and amyoplasia. *J Am Acad Orthop Surg* 2002; 10: 417–424.
- Kimber E. AMC: amyoplasia and distal arthrogryposis. *J Child Orthop* 2015; 9: 427–432.
- Rahman T, Sample W, Jayakumar S, et al. Passive exoskeletons for assisting limb movement. *J Rehabil Res Dev* 2006; 43: 583–590.
- Ezaki M. An approach to the upper limb in arthrogryposis. *J Pediatr Orthop* 2010; 30: 57–62.
- Van Heest AE. Arthrogryposis. In: Laub DR Jr (ed.) *Congenital anomalies of the upper extremity*. Boston, MA: Springer US, 2015, pp.305–315.
- Hall JG. Arthrogryposis (multiple congenital contractures): diagnostic approach to etiology, classification, genetics, and general principles. *Eur J Med Genet* 2014; 57: 464–472.
- Van Heest AE, James MA, Lewica A, et al. Posterior elbow capsulectomy with triceps lengthening for treatment of elbow extension contracture in children with arthrogryposis. *J Bone Joint Surg Am* 2008; 90: 1517–1523.
- Lahoti O and Bell MJ. Transfer of pectoralis major in arthrogryposis to restore elbow flexion. *Bone Joint J* 2005; 87: 858–860.
- Dunning AG and Herder JL. A review of assistive devices for arm balancing. In: *IEEE International conference on rehabilitation robotics*, Seattle, WA, USA, 24–24 June 2013, pp.1–6. Available at: <http://ieeexplore.ieee.org/document/6650485/> (accessed 15 February 2018).
- Krokmark A-K, Kimber E, Jerre R, et al. Muscle involvement and motor function in amyoplasia. *Am J Med Genet A* 2006; 140A: 1757–1767.
- Banala SK, Agrawal SK, Fattah A, et al. Gravity-balancing leg orthosis and its performance evaluation. *IEEE Trans Robot* 2006; 22: 1228–1239.
- Kooren PN, Dunning AG, Janssen MMHP, et al. Design and pilot validation of A-gear: a novel wearable dynamic arm support. *J Neuroeng Rehabil* 2015; 12: 1–12.
- Lin PY, Shieh WB and Chen DZ. A stiffness matrix approach for the design of statically balanced planar articulated manipulators. *Mech Mach Theory* 2010; 45: 1877–1891.
- Lustig MP, Dunning AG and Herder JL. Parameter analysis for the design of statically balanced serial linkages using a stiffness matrix approach with Cartesian coordinates. In: *14th IFToMM world congress*, Taipei, Taiwan, 25–30 October 2015, pp.122–129. Available at: <https://www.researchgate.net/publication/286780292> (accessed 15 February 2018).
- Dunning AG and Herder JL. A close-to-body 3-spring configuration for gravity balancing of the arm. In: *International conference on rehabilitation robotics (ICORR)*, Nanyang, Singapore, 11–14 August 2015, pp.464–469. Available at: <http://ieeexplore.ieee.org/document/7281243/> (accessed 15 February 2018).
- Zee M De, Hansen L, Wong C, et al. A generic detailed rigid-body lumbar spine model. *J Biomech* 2007; 40: 1219–1227.
- Veeger HEJ, Van der Helm FCT, Van der Woude LHV, et al. Inertia and muscle contraction parameters for musculoskeletal modelling of the shoulder system. *J Biomech* 1991; 24: 615–629.
- Van der Helm FCT, Veeger HEJ, Pronk GM, et al. Geometry parameters for musculoskeletal modelling of the shoulder system. *J Biomech* 1992; 25: 129–144.
- Veeger HEJ, Yu B, An KN, et al. Parameters for modelling the upper extremity. *J Biomech* 1997; 30: 647–652.
- Andersen MS, Damsgaard M, MacWilliams B, et al. A computationally efficient optimisation-based method for parameter identification of kinematically determinate and over-determinate biomechanical systems. *Comput Meth Biomech Biomed Eng* 2010; 13: 171–183.
- Rasmussen J, De Zee M, Damsgaard M, et al. A general method for scaling musculo-skeletal models. In: *10th International symposium on computer simulation in biomechanics*, Cleveland, OH, USA, 28–30 July 2005, pp.1–2. Available at: [http://vbn.aau.dk/en/publications/a-general-method-for-scaling-musculoskeletal-models\(1d822890-b6a5-11db-8b72-000ea68e967b\).html](http://vbn.aau.dk/en/publications/a-general-method-for-scaling-musculoskeletal-models(1d822890-b6a5-11db-8b72-000ea68e967b).html) (accessed 15 February 2018).
- Damsgaard M, Rasmussen J, Christensen ST, et al. Analysis of musculoskeletal systems in the anybody modelling system. *Simul Model Pract Theory* 2006; 14: 1100–1111.
- Rasmussen J, Damsgaard M and Voigt M. Muscle recruitment by the min/max criterion – a comparative numerical study. *J Biomech* 2001; 34: 409–415.
- Rosen J, Perry JC, Manning N, et al. The human arm kinematics and dynamics during daily activities – toward a 7 DOF upper limb powered exoskeleton. In: *IEEE 12th International conference on advanced robotics*, Seattle, WA, USA, 17–20 July 2005, pp.532–539. Available at: <http://ieeexplore.ieee.org/document/1507460/> (accessed 15 February 2018).
- Andersen MS, Damsgaard M and Rasmussen J. Kinematic analysis of over-determinate biomechanical

- systems. *Comput Methods Biomech Biomed Eng* 2009; 12: 371–384.
30. Nef T, Guidali M and Riener R. ARMin III – arm therapy exoskeleton with an ergonomic shoulder actuation. *Appl Bionics Biomech* 2009; 6: 127–142.
  31. Herder JL, Vrijlandt N, Antonides T, et al. Principle and design of a mobile arm support for people with muscular weakness. *J Rehabil Res Dev* 2006; 43: 591–604.
  32. Rahman T, Sample W, Seliktar R, et al. Design and testing of a functional arm orthosis in patients with neuromuscular diseases. *IEEE Trans Neural Syst Rehabil Eng* 2007; 15: 244–251.
  33. Buckley MA, Yardley A, Johnson GR, et al. Dynamics of the upper limb during performance of the tasks of everyday living – a review of the current knowledge base. *Proc Inst Mech Eng H: J Eng Med* 1996; 210: 241–247.
  34. Zhou L, Bai S, Andersen MS, et al. Modeling and design of a spring-loaded, cable-driven, wearable exoskeleton for the upper extremity. *Model Identif Control* 2015; 36: 167–177.
  35. Hill AV. The heat of shortening and the dynamic constants of muscle. *Proc R Soc B Biol Sci* 1938; 126: 136–195.
  36. Garner BA and Pandy MG. Estimation of musculotendon properties in the human upper limb. *Ann Biomed Eng* 2003; 31: 207–220.
  37. Castro MN, Rasmussen J, Bai S, et al. On model validation using the reachable 3d space. In: *15th International symposium computer methods in biomechanics*, Edinburgh, UK, 9–11 July 2015, pp.1–2. Available at: [http://vbn.aau.dk/files/209330397/ISCSB2015\\_On\\_model\\_validation\\_using\\_reachable\\_3d\\_space\\_FiNAL.pdf](http://vbn.aau.dk/files/209330397/ISCSB2015_On_model_validation_using_reachable_3d_space_FiNAL.pdf) (accessed 15 February. 2018).